Agricultural Water Management 216 (2019) 196–205

Contents lists available at ScienceDirect

Agricultural Water Management

journal homepage: www.elsevier.com/locate/agwat

Applying high-resolution visible-channel aerial imaging of crop canopy to precision irrigation management

Assaf Chen*,[1], Valerie Orlov-Levin[1], Moshe Meron[1]

MIGAL Galilee Research Institute, Kiryat Shmona 11016, Israel

ARTICLE INFO

Keywords:
Canopy cover
Vegetation fraction
Green-red vegetation index (GRVI)
Precision irrigation
Remote sensing
Unmanned aerial vehicle (UAV)

ABSTRACT

Canopy cover (or vegetation cover) maps serve in irrigation management mainly to determine the primary evapotranspiration (ET) coefficient, as radiation interception and evaporative surface area are directly related to canopy cover. Crop size and development with time depends on water supply; therefore, crop canopy maps are tools for the detection of the spatial uniformity of irrigation systems. Several aerial scan campaigns were deployed in the Upper Galilee of Israel in the 2017 and 2018 growing seasons to follow up and evaluate the irrigation uniformity and crop coefficients of peanuts and cotton by RGB scans of a Phantom 4 multirotor unmanned aerial vehicle (UAV) and DJI Mavic-Pro UAV equipped with RGB and near-infrared (NIR) sensors. Foliage intensity and coverage were enhanced by a green-red vegetation index (GRVI), which is a normalized difference vegetation index (NDVI)-like process where the green channel replaced the NIR. The results demonstrated that the GRVI is suitable for the purpose of determining the vegetation cover. Furthermore, the GRVI yielded better results than the NDVI in recognizing phenological crop changes (especially senescence) and in detecting heterogeneity in field irrigation. Therefore, this research proves the applicability of a low-cost digital camera mounted on an easily accessible UAV for crop cover and actual, in-field, ET coefficients determination and irrigation uniformity evaluation.

1. Introduction

A lot of work has been done investigating plants' spectral reflectance in the visible and near-infrared part of the electromagnetic spectrum at different phenological stages. Understanding the single leaf's spectral response and the processes that occur on this level allows to apply this knowledge to the canopy level (Hatfield et al., 2008). Spectral indexes allow for better information extraction from remotely sensed data because they reduce the effects of soil, view angle, and topography, while enhancing the focus on the desired extracted feature (e.g., the vegetation indexes enhance the visibility of the vegetation) (Hunt et al., 2012). Multitude of vegetation indexes (VI) were introduced in order to evaluate plant's vigor and stress. While multiple VIs that use the ratio between the red and near-infrared (NIR) spectral wavebands (e.g., normalized difference vegetation index (NDVI), ratio vegetation index (RVI), soil adjusted vegetation index (SAVI)) (Huete, 1988; Jordan, 1969; Rouse et al., 1973; Tucker, 1979) are successful in reducing atmospheric radiance and transmittance (Hunt et al., 2011; Tucker, 1979), the red wavelengths are strongly absorbed by chlorophyll and therefore are less sensitive to changes in chlorophyll content (Gitelson et al., 1996, 2005; Hunt et al., 2011; Yoder and Waring, 1994). As the leaf area index (LAI) increases, apparent canopy chlorophyll content also increases regardless of the single-level leaf chlorophyll content, therefore these VIs are much more affected by LAI than by changes in chlorophyll at the canopy scale (Daughtry et al., 2000; Eitel et al., 2009; Hunt et al., 2011). Since chlorophyll is vital for the photosynthesis process, changes in chlorophyll levels can be linked to photosynthetic productivity, developmental (phenological) stages, and plant stress. Chlorophyll levels also correlate to green vegetation nitrogen levels – nitrogen shortage reduces leaf chlorophyll content, thus decreasing plant spectral absorption especially in the blue and red wavelengths, therefore increasing reflectance in these wavelengths (Gitelson et al., 2005; Haboudane et al., 2004; Hatfield et al., 2008; Hunt et al., 2012; Yoder and Waring, 1994). Nitrogen is a vital plant nutrient, most important for crop growth and yield.

On the other hand, the green wavelengths are more sensitive to high chlorophyll levels, since they are less absorbed by chlorophyll *a* and *b*, unlike the blue, red, and NIR wavelengths (Gitelson et al., 1996, 2005; Hunt et al., 2011; Yoder and Waring, 1994). Therefore, VIs using the green wavelength are capable of detecting changes in chlorophyll

* Corresponding author.
E-mail addresses: assafc@migal.org.il (A. Chen), valerieo@migal.org.il (V. Orlov-Levin), meron@migal.org.il (M. Meron).
[1] www.migal.org.il.

https://doi.org/10.1016/j.agwat.2019.02.017
Received 12 November 2018; Received in revised form 4 February 2019; Accepted 9 February 2019
Available online 15 February 2019
0378-3774/

contents at the leaf and canopy scale and are suitable to monitor plants' developmental stages and stress.

Gitelson et al. (Gitelson et al., 2002) found that the NIR reflectance band is less sensitive for determining the vegetation cover (or vegetation fraction—VF) for VF > 60% and showed that a VI using the green–red–blue wavelengths have a linear relationship to VF, with an accuracy level of up to 90%. They showed that in wheat, when VF is between 50 and 100%, the green wavelength is most sensitive to changes in the vegetation cover (while the blue, red, and NIR wavelengths are insensitive to changes in the vegetation cover).

Adamsen et al. (Adamsen et al., 1999) measured "Greenness" of wheat plants throughout the cropping season using a digital camera, a hand-held radiometer, and chlorophyll meter. They found that the green to red (G/R) spectral wavelengths ratio index is sensitive to the amount of greenness of the plant: it is less than 1 in the beginning and at the end of the growing season, and above 1 at midseason (Adamsen et al., 1999; Kanemasu, 1974). The G/R index obtained from an uncalibrated digital camera was more sensitive to plant senescence than the chlorophyll meter, and on par with the NDVI index obtained from the hand-held radiometer, thus proving that moderate cost digital cameras can be used to monitor crop senescence (Adamsen et al., 1999). Kanemasu (Kanemasu, 1974) concluded that the G/R ratio may serve as a benchmark for crop growth, phenological stages, and for indicating the VF.

Another VI that is based on the G/R ratio is the green-red vegetation index (GRVI) that is defined according to Eq. (1):

$$GRVI = (\rho green - \rho red)/(\rho green + \rho red) \quad (1)$$

Motohka et al. (Motohka et al., 2010) evaluated the use of the GRVI as a phenological indicator. They concluded that the GRVI index can differentiate between green vegetation (index above 0), water and snow (index around 0), and soils (index below 0). Furthermore, they demonstrated that the GRVI (unlike the NDVI) is sensitive to leaf color change (leaf greening and autumn coloring). They suggested using the threshold of GRVI = 0 as a site-specific threshold for monitoring phenological changes and the GRVI index as an indicator for plant disturbances, and comparing between different ecosystem types (Motohka et al., 2010).

Remote sensing for crop management aims at providing spatial and spectral information for crop classification, crop condition, yield forecast, and weed/disease detection and management. Current satellite-based remotely sensed products can cover large areas, but they are limited by both their temporal (revisit time – 2 and 5 days for Venus and Sentinel-2 satellites, respectively) and spatial (pixel size – 5–10 m for Venus and Sentinel-2, respectively) resolutions, when compared to unmanned aerial vehicle (UAV). One of satellite imaging's challenges is dealing with pixels that have multiple objects with different spectral signatures (e.g., plants and soil). Such pixels are called mixed-pixels. UAV, imaging high spatial resolution, produces mixed-free pixels, therefore making vegetation detection and differentiation an easier task. Similarly, high spatial resolution allows for a precise estimation of the vegetation cover fraction.

A basic method for irrigation scheduling is factoring the potential evapotranspiration (PET), computed from measured radiation, wind speed, air temperature, and relative humidity, with a crop-specific coefficient (Kc)) as widely accepted and formulated by the FAO #56 publication (Testa et al., 2011). Crop coefficients are provided by diverse methods, such as empirical conclusions from field experiments, degree-day-based seasonal functions, experts' recommendations, and the FAO #56 publication Kc library, or by field-specific measurements. According to the Penman-Monteith equation, solar radiation comprise about 85% of the evapotranspiration (ET) driving energy received by the crop canopy (Testa et al., 2011), and intercepted solar radiation is directly proportional to the light interception (LI) (Green et al., 2003; Johnson et al., 2000; Meron et al., 1989). Further, since LI is directly proportional to crop canopy cover, Kc can be fitted to the field- and plot-specific dimension by measuring crop cover. Therefore, VF can be used as Kc. Aerial survey-derived VFs are directly proportional to cover, (Meron et al., 2006) thus digital aerial photography provides an efficient method for Kc determination (Campillo et al., 2008).

Precision irrigation can be defined as matching water application to crops' need in space, time and amount. Variable rate water application to achieve that is feasible with solid set systems using modern controllers and in variable rate center pivot or lateral move irrigation machines, all available in the open market. However, such application needs spatial and temporal crop water status information in sufficient resolution and accuracy, attainable mainly by aerial sensing and imagery (Haghverdi et al., 2015; Nahry et al., 2011; Zhang et al., 2011). Digital aerial photography became affordable and popularized with the appearance in the open market of low cost, high performance small sized unmanned aerial vehicles (UAV) carrying high resolution digital cameras, in contrast with the former less accessible human flown aerial photography. Testing of these new enabling technologies for precision irrigation information acquisition is obviously needed. Such a technology is presented herein.

The main objectives of this study were to test the ability of an inexpensive RGB camera mounted on an inexpensive UAV to determine vegetation cover and vigor of the canopy at a large-scale whole-field resolution and to investigate whether vegetation cover and vigor patterns can be utilized as indicators for irrigation water uniformity, and as such, feedback information for precision water application at variable rate irrigation (VRI) systems. Another objective of this study was to compare the efficiency of an RGB- based VI with that of the well-known NDVI, both in UAV-based high spatial resolution cameras and via satellite imaging.

2. Materials and methods

2.1. UAV imaging system

DJI Phantom 4 quadcopter UAV was used as the flying platform. The UAV is equipped with a built-in RGB camera with a 4000 × 3000 pixel 4 K resolution CMOS sensor, a 20 mm (35 mm eq.) lens with field of view (FOV) of 94°, in a 3-axis stabilized gimbal (https://www.dji.com/phantom-4/info). The UAV was flown using Pix4D Capture pre-programmed flightpath control. The Parrot Sequoia multispectral sensor was used in order to compare NDVI with GRVI. The Parrot Sequoia sensor consists of five downward-looking image sensors: a Visible 16 MegaPixel (MP) (RGB) with a definition of 4608 × 3456 pixels and four 1.2 MP: Green (550 nm), Red (660 nm), Red Edge (735 nm), and Near-infrared (790 nm) bands, 1280 × 960 pixels (https://www.parrot.com/business-solutions-us/parrot-professional/parrot-sequoia#parrot-sequoia-pix4d-precise-data-brings-accurate-analysis). The sensor was mounted on a DJI Mavic-Pro small-size, foldable-rotor quadcopter UAV. Sensors were factory pre-calibrated. Parrot Sequoia sensor was recalibrated before each campaign using a white balance reference target. Phantom 4 RGB sensor's white balance setting was set to sunny. No other color or style enhancements were made to the obtained images.

2.2. Flight campaigns

Flight campaigns were conducted in three test sites: the Gadot center pivot test site (33°2′22.91″ N, 35°38′0.43″ E), the Havat Gadash field crops experimental farm (33°10′56.24″ N, 35°35′5.78″ E), and the Hagoshrim lateral move test site (33°11′57.75″ N, 35°38′19.15″ E), all three located in the Upper Galilee region in the northern part of Israel. The area has a Mediterranean climate, characterized by wet, mild winters with mean minimum and maximum temperatures of 7 and 14 °C, respectively, and hot, dry summers with mean minimum and maximum temperatures of 19 and 32 °C respectively. Annual winter rainfall is in the range of 400–600 mm, while summer crops utilize

Table 1
Cumulative evapotranspiration (ET), irrigation water applied, and crop-specific coefficients (Kc) in the peanut irrigation experiment, Havat Gadash 2017. Highlighted Kcs' correlate to Havat Gadash flight campaign dates (Table 2).

	Date	Cumulative ET (mm)*	Irrigation (mm)	Cumulative Irrigation (mm) *	Kc **
Uniform irrigation	08/05/2017	43	30	30	0.70
	04/06/2017	213	40	70	0.33
	13/06/2017	272	40	110	0.40
	29/06/2017	384	45	155	0.40
	06/07/2017	431	45	200	0.46
	12/07/2017	474	45	245	0.52
0.7 Kc Irrigation	19/07/2017	43	37	37	0.86
	27/07/2017	96	37	74	0.77
	03/08/2017	143	37	111	0.78
	10/08/2017	186	37	148	0.80
	19/08/2017	240	37	185	0.77
	30/08/2017	308	37	222	0.72
	10/09/2017	369	37	259	0.70
	24/09/2017	434	40	299	0.69

* Cumulative amounts recalculated for the two experimental stages.
** Kc calculated as cumulative irrigation divided by cumulative ET.

80–120 mm of winter soil water storage for the initial growth periods.

At the Havat Gadash, peanuts cv *Hanoch* were sown on 1 May 2017 and irrigated uniformly by an experimental lateral move, starting on 8 May (Table 1). PET was calculated according to the Penman–Monteith formula, based on meteorological field data. Kc was calculated as cumulative irrigation divided by cumulative ET. Four differential irrigation treatments were performed starting on 19 July (Fig. 1). The Kc (70%) treatment yielded the highest crop weight per area (5.86 ton/hectare; more than 0.7 ton/hectare compared to the rest of the treatments), implying optimal water application and water use, and was selected for ground truth validation – comparing field measured Kc with aerial imagery calculation of VF. Experimental plots were four 12 × 25 m plots, side by side in four replicates (Fig. 1). Seven flight campaigns were conducted at midday, at 10–50 m altitude and pixel spatial resolution of 0.006–0.02 m (Table 2). Crop cover did not reach full cover during the first two campaigns (25 June, 17 July). Full cover is reached when there are less than 20% pixels that are classified as bare soil.

The field at the Gadot center pivot test site was cultivated with cotton crop, sown on 4 April 2017. The field was irrigated at eight-day intervals beginning from 3 June. Two flight campaigns were conducted on 5 July and 24 August, when the crop had already reached full cover.

Table 2
Havat Gadash flight campaigns' information.

Date	Time	Elevation (m)	Spatial resolution (m)	Days from sowing	GRVI calculated vegetation fraction - VF (%)
Havat Gadash					
25/06/2017	10:55	10	0.0066	55	46
17/07/2017	10:30	10	0.0066	77	87
03/08/2017	10:30	50	0.022	94	99
07/09/2017	13:15	15	0.0075	129	94
11/09/2017	10:30	50	0.022	133	95
19/09/2017	14:10	15	0.0075	141	89
27/09/2017	16:00	10	0.0066	149	87
Gadot Test Site					
05/07/2017	11:00	50	0.022	92	100
24/08/2017	10:00	50	0.002	142	100
Hagoshrim Test Site					
17/06/2018	13:00	100	0.043	98	100
26/06/2018	13:00	100	0.043	107	100
NDVI vs. GRVI (DJI Mavic-Pro)					
10/10/2017	11:35	40	0.0095 (RGB) 0.0373 (NIR)	163	N/A

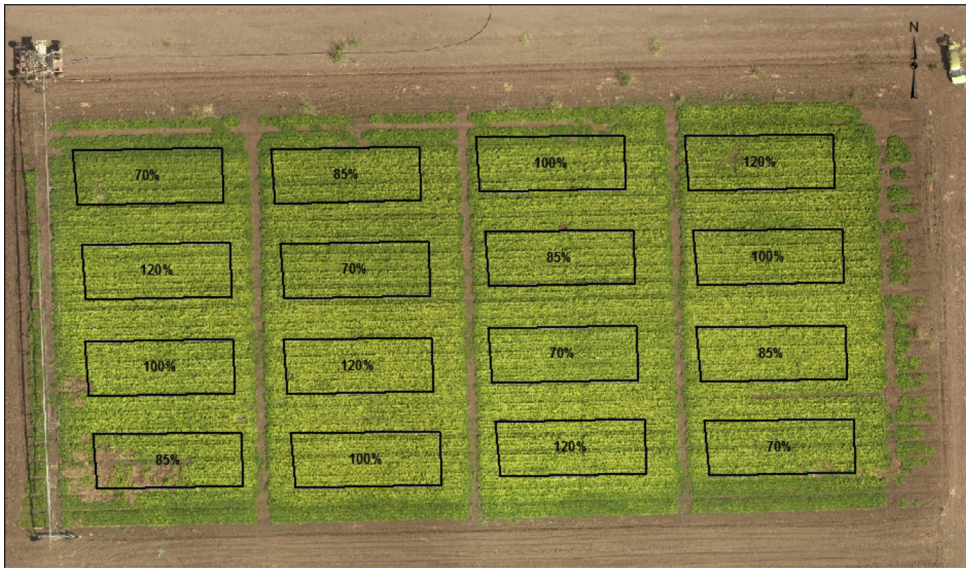

Fig. 1. Havat Gadash peanut field with the layout of the four irrigation treatments indicated. Image was taken on the September 11, 2017 flight campaign.

The flights were conducted at midday, at 50 m altitude and pixel spatial resolution of 0.02 m (Table 2). The field at the Hagoshrim lateral move test site was cultivated with cotton crop, sown on 1 1 March 2018. The field was irrigated at five-day intervals beginning from 24 May. Two flight campaigns were conducted on 17 and 26 June, when the crop had already reached full cover. The flights were conducted at midday, at 100 m altitude and pixel spatial resolution of 0.043 m (Table 2).

Flight courses were created with the Pix4Dcapture software, which was also used to automatically pilot the DJI Phantom 4 UAV according to the flight path. An overlap percentage of 70–80% was chosen in order to ease the task of mosaicking.

In order to compare NDVI and GRVI, a flight campaign using the DJI Mavic-Pro UAV was conducted in the peanut field at the Havat Gadash experimental farm on October 10, 2017, twelve days before the end of the growing season (Table 2). The Parrot Sequoia multispectral sensor was used to create the NDVI, while the RGB camera was used to create the GRVI.

2.3. Data processing

The images collected in each flight campaign were mosaicked and georeferenced using the Pix4Dmapper software. The ArcGIS 10.5 georeferencing tools were used for fine adjustments.

VF was calculated using ArcGIS 10.5, calculating the histogram of the GRVI products. Pixels with GRVI values greater than 0 were classified as vegetation, according to Motohka et al. (2010).

Sentinel-2 Level-2 A atmospherically corrected images of the Gadot test site from 29 August 2017 were acquired courtesy of the Copernicus Open Access Hub. Venus satellite Level-1 radiometrically corrected and top-of-atmosphere reflectance images of the Hagoshrim test site from 17 June 2018 were acquired courtesy of CNES (French government space agency) ISA (Israeli space agency) and the scientific center at the Ben-Gurion University, Israel. Several VIs were created and compared to the UAV images, in order to check whether it is possible to use Sentinel-2 and Venus satellite imaging (with spatial resolution of 10 and 5 m, respectively) to determine irrigation uniformity issues. The following VIs were checked: NDVI (Tucker, 1979), green normalized difference vegetation index (GNDVI) (Gitelson et al., 1996), and GRVI (Motohka et al., 2010; Tucker, 1979). UAV images were compared to similar date satellites images for the sake of proper comparison (same day as Venus, and 4 days apart from Sentinel-2 imagery).

All images taken with the DJI Phantom-4 UAV built in camera equipped with a gimbal assuring vertical nadir direction, were acquired close to midday (when the sun is close to zenith), taking images of flat agricultural surfaces, thus limiting bidirectional reflectance distribution function (BRDF) complication. Furthermore, at the height of UAV image acquisition (10–100 m) and for the purpose of analyzing RGB color space no special calibration or atmospheric correction was applied beyond the standard factory calibration.

3. Results

3.1. Havat Gadash experimental farm campaign

The RGB images (Fig. 2A,C) have high spatial resolution (0.0066 m, see Table 2), allowing the differentiation of crop from soil. Negative GRVI values were classified as non-vegetation (i.e. soil), and positive GRVI values were classified as vegetation. The VFs determined according to the GRVI images' histograms were 46% and 87% (Fig. 3A,B respectively): whereas, the VF can be determined as 1 minus the intersection value of the cumulative GRVI graph with the Y axis in Fig. 3, The field calculated Kc for the campaign dates (Table 1: highlighted Kcs) of 40% and 86% were in-par with the image calculated VFs of 46% and 87%, respectively, validating the VF calculations.

The GRVI images revealed crop phenological stages: whereas 9% of the pixels' GRVI values in the image taken 55 days from sowing were below zero and outside of the "soil curve" pixels group (Fig. 3A), only 3% of the pixels' GRVI were below zero and outside of the "soil curve" pixels group in the later image at 77 days from sowing (Fig. 3B). These pixels that don't belong to either the soil or vegetation classified groups, were classified as non-vegetation pixels (due to their negative GRVI value), but could also be classified as vegetation in early phenological stages with G/R ratio values less than 1 (negative GRVI value yields G/R ratio below 1)—indicative of the beginning of the growing season. Furthermore, the "vegetation curve" in the later image is further away from the Y-axis compared to the chronologically earlier image (Fig. 3A,B) with higher positive GRVI values, indicative of healthy and vital vegetation suitable to the midseason phenological stage.

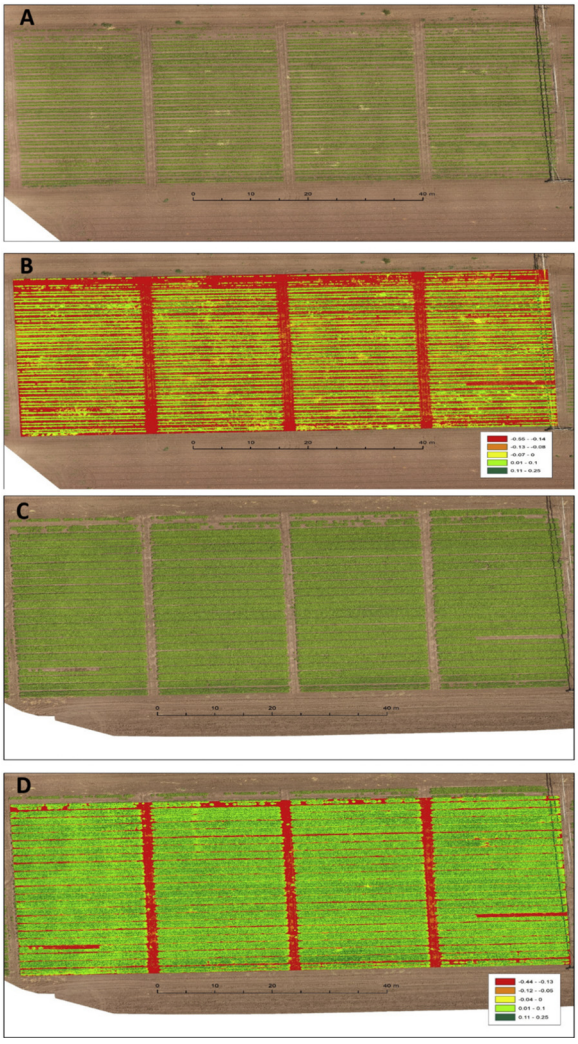

Fig. 2. RGB (A + C) and green-red vegetation index (GRVI) (B + D) images of the peanut field in Havat Gadash experimental farm on 25 June (A + B, 55 days from sowing) and on 17 July (C + D, 77 days from sowing) (For interpretation of the references to colour in this figure legend, the reader is referred to the web version of this article).

As can be seen in Table 2 – crop cover reaches almost 100% (full cover) by the third flight campaign, but in later campaign there is a drop in VF. The reason behind this is due to pest damage (wild boars; see Fig. 1, bottom left corner). Images are not shown.

3.2. Comparison between NDVI and GRVI

Since there were two different sensors measuring the NDVI and the GRVI (Section 2.3), the spatial resolution of the NDVI was lower (pixel size of 0.0373 m) than that of the GRVI (0.0095 m), thus enabling

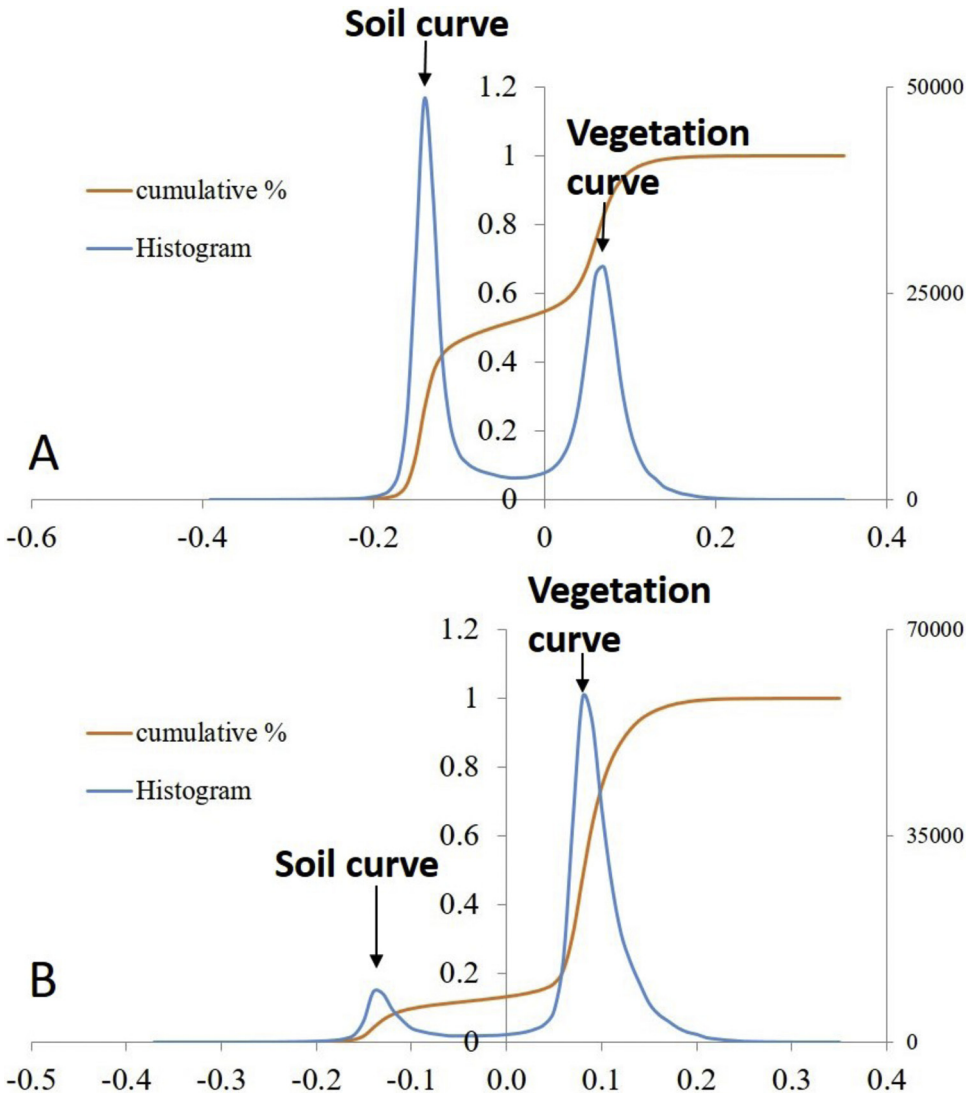

Fig. 3. Histogram of the GRVI images of the peanut field in Havat Gadash experimental farm on 25 June (A, 55 days from sowing) and on 17 July (B, 77 days from sowing). Cumulative values are presented on major Y-axis and histogram value are presented on secondary Y-axis.

sharper GRVI imagery. The image was taken toward the end of the season, depicting plants in different stages of senescence. The RGB image was classified into specific classes (bare soil, dead vegetation, light green vegetation, dark green vegetation) using supervised classification aided by Image-Pro software (http://www.mediacy.com/imagepro) "Smart Segmentation" algorithm (Fig. 4B). Table 3 presents the total area for each defined class, for the classified RGB, GRVI and NDVI images. As seen in Table 3, the GRVI classification is more similar to the RGB classification, especially in detecting light and dark green vegetation, differentiating between healthy (dark green) and stressed (i.e. in senescence) plants (light green). As can be seen in Fig. 4, the GRVI captured plant senescence better than the NDVI: changes in plant color from green to yellow are depicted more accurately in the GRVI image than in the NDVI image. Greener vegetation (depicted in the RGB image Fig. 4A,B) has higher GRVI values (Fig. 4C). On the other hand, the NDVI image (Fig. 4D) did not capture the color differences between plants that are visible in the RGB image (Fig. 4A,B). The NDVI values are very high for most pixels (0.81-0.92, Fig. 4D), indicating saturation of the NDVI values, probably due to high LAI values (Daughtry et al., 2000; Eitel et al., 2009; Hunt et al., 2011). It is probable that the differences in pixel resolution are also responsible for the accuracy differences. Regardless, for the purpose of vegetation classification and vigor analysis, the use of RGB VI is preferable to that of the NDVI.

3.3. Gadot test site campaign

The images of the Gadot pivot irrigated cotton crop were taken after the crop had reached full canopy cover (Fig. 5A,C). A closer look at the GRVI images reveals "sector" lines, indicating differences in plant vigor (Fig. 5B,D). The "sector" patterns are indicative of ununiformed irrigation, due to intermittent pivot movement: the "greener" areas probably received more irrigation, due to lower pivot speed. This could have resulted from physical obstacles, uneven ground, malfunctioning pivot control, etc. Whereas these "sectors" are noticeably visible in the GRVI image, it is impossible to notice them in the RGB image. Therefore, using the GRVI in this case is crucial in order to detect irrigation uniformity, irrigation malfunctions, and other subtle disturbances.

3.4. Sentinel-2 satellite VI of the Gadot test site

The NDVI and GNDVI images are pretty similar, showing high values homogenously throughout the whole field, except for the middle left corner (Fig. 6A,B). The GRVI image is more heterogeneous, showing patches of low values that are correlated to the UAV high-resolution GRVI image's patches (Figs. 5D and 6 C), indicative of the field's

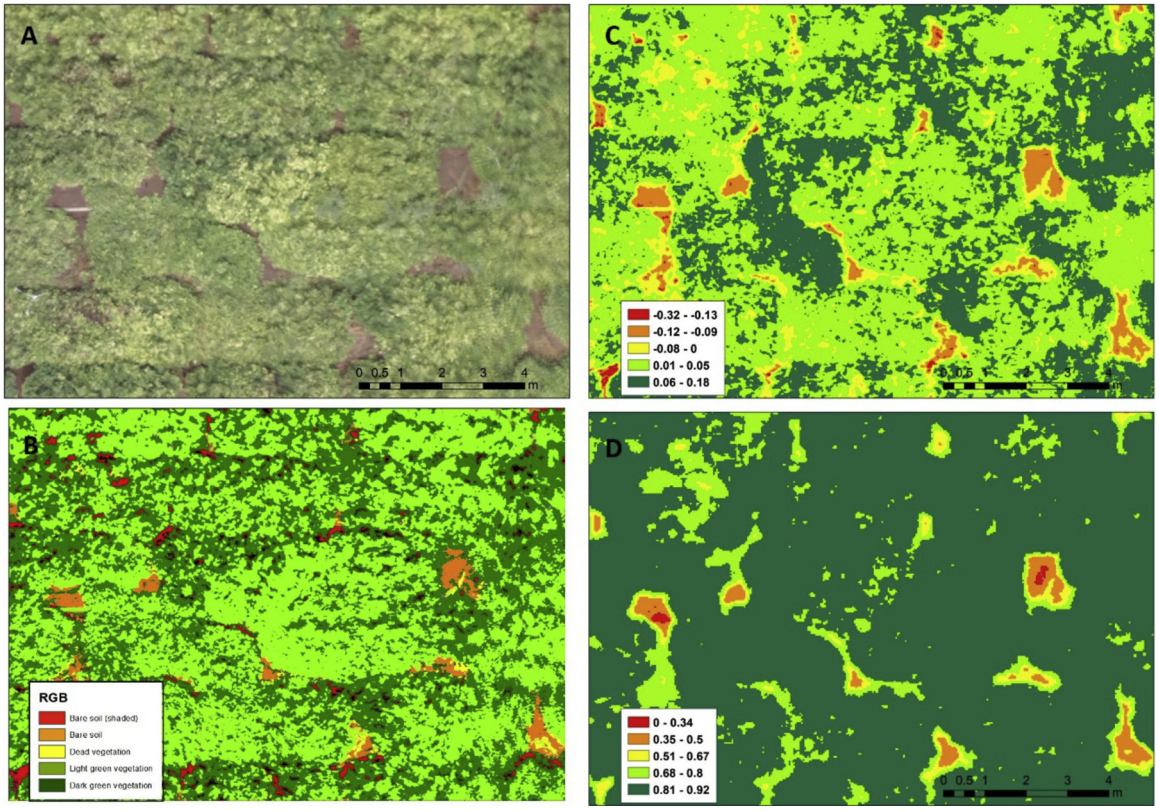

Fig. 4. RGB (A); classified RGB (B); GRVI (C) and normalized difference vegetation index (NDVI) (D) zoom-in images of the peanut field at Havat Gadash experimental farm.

Table 3
Land cover classes and total area for RGB, GRVI and NDVI images of the peanut field at Havat Gadash experimental farm.

Class	# pixels RGB	Total area (%) RGB	# pixels GRVI	Total area (%) GRVI	# pixels NDVI	Total area (%) NDVI
Bare soil	147,886	4%	106,035	3%	62,628	1%
Dead vegetation	38,912	1%	283,692	7%	74,555	2%
Light green vegetation	1,930,192	52%	2,173,767	56.5%	407,763	11%
Dark green vegetation	1,628,823	43%	1,290,563	33.5%	3,309,329	86%

heterogeneous plant vigor and ununiformed irrigation. The GRVI is therefore better at presenting the real crop vigor situation. Whereas the saturation of red reflectance at intermediate to high chlorophyll values is well known (Gitelson et al., 2005; Kanemasu, 1974) and is typical of NDVI, it is surprising to see that the GNDVI was also saturated and did not show field's heterogeneity.

3.5. Hagoshrim test site campgain

The images of the irrigated cotton at the Hagoshrim lateral move irrigation system were taken after the crop had reached full canopy cover albeit it is possible to see within the field bare soil lines that were created due to the pivot's wheels movement (Fig. 7C). A closer look at the GRVI images reveals lines, indicating differences in plant vigor (Fig. 7A,B). These patterns are indicators for ununiformed irrigation. There are both horizontal and vertical lines (Fig. 7A,B). The horizontal lines are indicative of intermittent pivot movement: Similar to the Gadot test site, the denser biomass (greener) areas probably received more irrigation, due to lower pivot speed. The vertical lines are indicative of differences in the amount of water delivered by the different sprinklers on board the pivot, and/or differences in the amount of overlap of irrigation between neighboring sprinklers. The heterogeneity in field's plant vigor enhances as a function of time, indicative of an irrigation machine related persistent operation malfunction that is responsible for the ununiformed irrigation. On the practical level, such maps can be shown to the operator (and in fact has been shown) in order to readjust lateral water distribution of the machine, and to identify and remove obstacles in machine movement along the travel path.

3.6. Venus satellite VI of the Hagoshrim test site

Similarly to the findings of the Sentinel-2 satellite at the Gadot campaign (Fig. 6), the NDVI and GNDVI images of Venus satellite (Fig. 8A,B) are pretty similar, showing lower values of field variability, when compared to the GRVI image (Fig. 8C). The vertical lines can be seen in all images, albeit most clearly in the GRVI image. Horizontal lines cannot be identified in any of the compared VI. The GRVI image is more heterogeneous, showing patches of low values that are correlated to the UAV high-resolution GRVI image's patches (Figs. 7A and 8 C). Therefore once more confirming that the GRVI is better than NDVI and GNDVI at presenting the real crop vigor situation.

4. Discussion

Evaluating crop cover during the beginning of the growing season with the aid of UAVs as described in this research can support and validate farmer's irrigation decision making process. Field irrigation

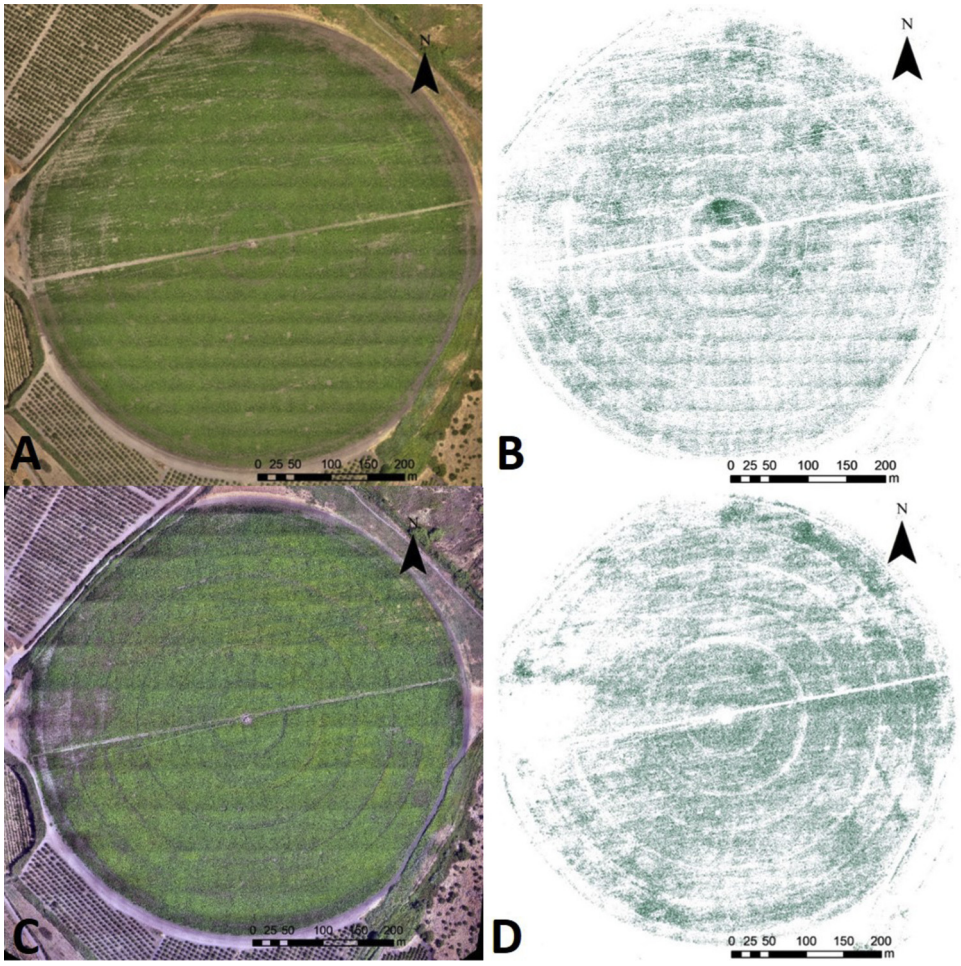

Fig. 5. RGB (A + C) and GRVI (B + D) images of the cotton field in Gadot test site on 5 July (A + B) and on 24 August (C + D).

depends on crop cover ratio, therefore up until the crop reaches full cover, it is necessary to re-evaluate crop cover at short time intervals in order to optimize irrigation water quantities. The technique proposed in this research offers an affordable and accurate solution. We propose conducting a UAV flight campaign a day before the scheduled irrigation in order to determine the current field's crop cover ratio, thus aiding the farmer in determining crop specific coefficient. An aerial survey should be conducted for every irrigation zone. In case the zone is very big, it is possible to sample only some parts of the whole area, based on the field's inherent heterogeneity (e.g. soil texture, soil type, soil water content, apparent soil electrical conductivity), and previous flight campaigns wherein crop cover heterogeneity was observed. Such sampling is beyond the scope of this paper, however it should be noted that the proposed techniques for crop cover estimation and crop heterogeneity detection can be integrated into other existing techniques that aim to improve the design of irrigation systems (Fortes et al., 2015). VRI systems can use crop cover ratio findings and heterogeneity in plant vigor in order to construct irrigation maps according to plants' water demands and to better prescribe variable irrigation rates according to plant size and cover ratio.

Even though much better, more accurate (and more expensive) sensors exist in the open market, we argue that for the purpose of

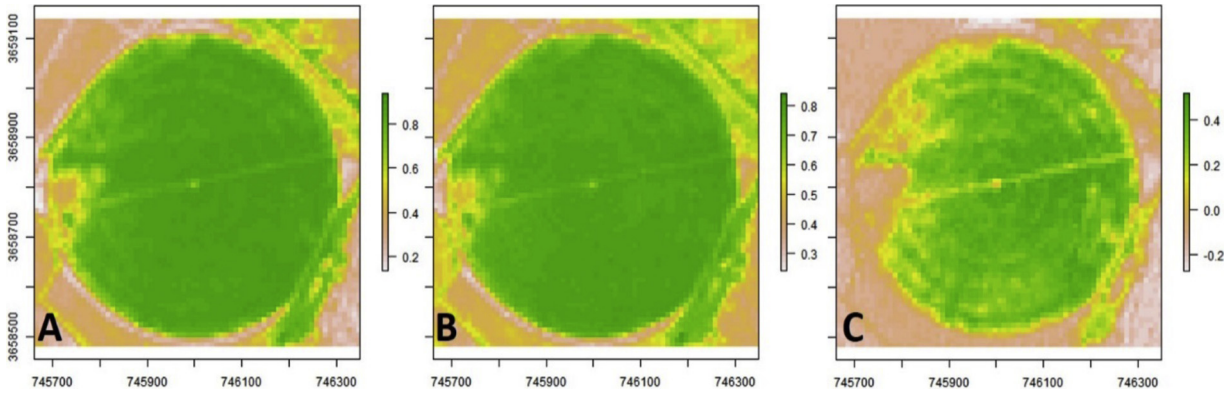

Fig. 6. NDVI (A); green normalized difference vegetation index (GNDVI) (B); and GRVI (C) vegetation indexes based on a Sentinel-2 imagery of the cotton field in Gadot test site from 29/08/2017 (For interpretation of the references to colour in this figure legend, the reader is referred to the web version of this article).

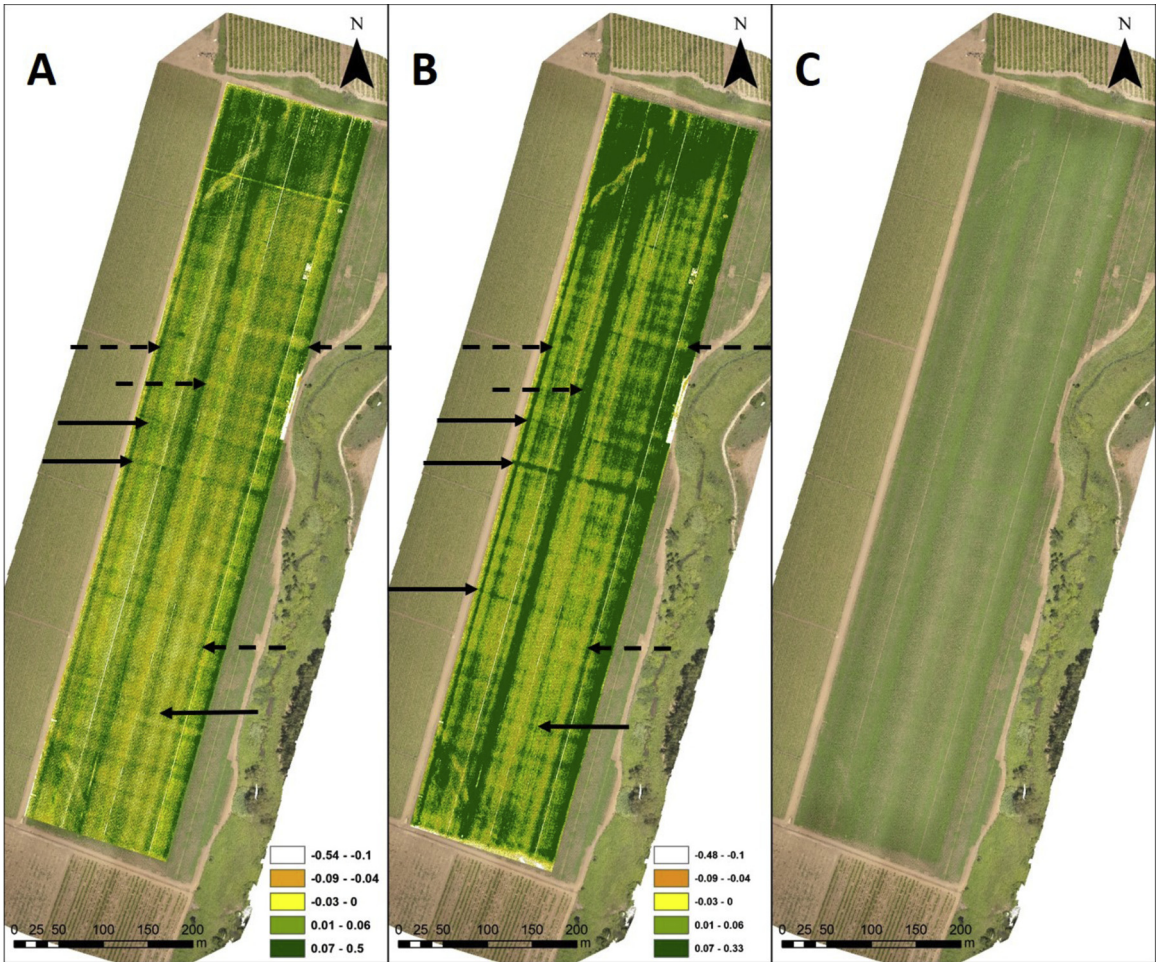

Fig. 7. GRVI (A + B) and RGB (C) images of the cotton field in Hagoshrim test site on 17 June (A) and on 26 June (B + C). Dashed arrows point to vertical vegetation lines; solid arrows point to horizontal vegetation lines.

determining crop cover ratio, utilizing affordable CMOS sensors such as were used in this research is adequate. Very high spatial resolution is paramount: it cancels the problem of mixed-pixels, and allows to obtain pure pixels of vegetation and bare soil, thus enabling to distinguish between bare soil and vegetation.

It is possible to differentiate soil from crop cover using raw RGB images (Fig. 2A,C). However, in order to quantify the ratio of crop cover to bare soil, it is necessary to classify these classes. Such a classification from RGB image is very complex, since there are 256^3 options of color combinations for each pixel. Converting the RGB image into a vegetation index simplifies the classification task tremendously. As Motohka et al. (Motohka et al., 2010) concluded, the GRVI is very suitable for such a task, wherein GRVI index values of above zero can be classified as green vegetation (Figs. 2B,D, 3). Furthermore, as shown in the results, the GRVI was sensitive to differences in crop's plant vigor, as expressed in chlorophyll composition and intensity, and in the number of pixels with negative, close to zero GRVI values at various phenological stages (Figs. 2,3), thus it could potentially be used in some crops as an indicator in determining phenological stages, and as a benchmark for phenological stages transitioning, such as senescence in groundnuts in this study. The GRVI also proved to be superior to the NDVI in detecting plant vigor, senescence, and irrigation uniformity (Figs. 4–6).

Detecting irrigation water uniformity is crucial for the purpose of optimizing water use and crop yields. Our results demonstrate that specifically in pivot irrigation, it is possible to detect heterogeneity in plant vigor that are caused due to abnormal pivot movement. The "sectors" that are perpendicular to the pivot's advancement direction, or horizontal lines in lateral moves, are indicative for slower pivot speed and over irrigation (Figs. 5,7); denser vegetation lines formed at the direction of the machine's advancement (vertical lines) are indicative of inherent problems in the sprinkler system calibration: overwatering / under-watering; distance between sprinklers; sprinklers' overlap due to the height of the sprinkler from the ground (Fig. 7). High spatial resolution UAV images are superior to the lower resolution satellite imaging in finding the "fine" lines that demarcate the field's heterogeneity (Figs. 5–8): whereas some of the lines were identified by the satellites' GRVI, it gave a rough idea towards understanding differences of plant vigor within the field's scale. In order to further analyze the intricacies of the field's heterogeneity it is necessary to get a closer look via UAV or other higher spatial resolution devices. Still, it was proven that satellite imaging can provide valuable information on large spatial scales regarding the field's plant vigor heterogeneity that can be further investigated on finer scales upon demand.

5. Conclusions

In this study, the ability of a high-resolution RGB imaging to determine vegetation cover and vigor at the canopy scale at whole-field resolution was evaluated, using an RGB VI, namely, the GRVI. It was concluded that the GRVI is suitable for determining vegetation cover, distinguishing between vegetation and other land covers (such as soil and dead vegetation, Fig. 2). The VF can be accurately measured and used by the farmer "on the spot" in order to directly define the Kc. It

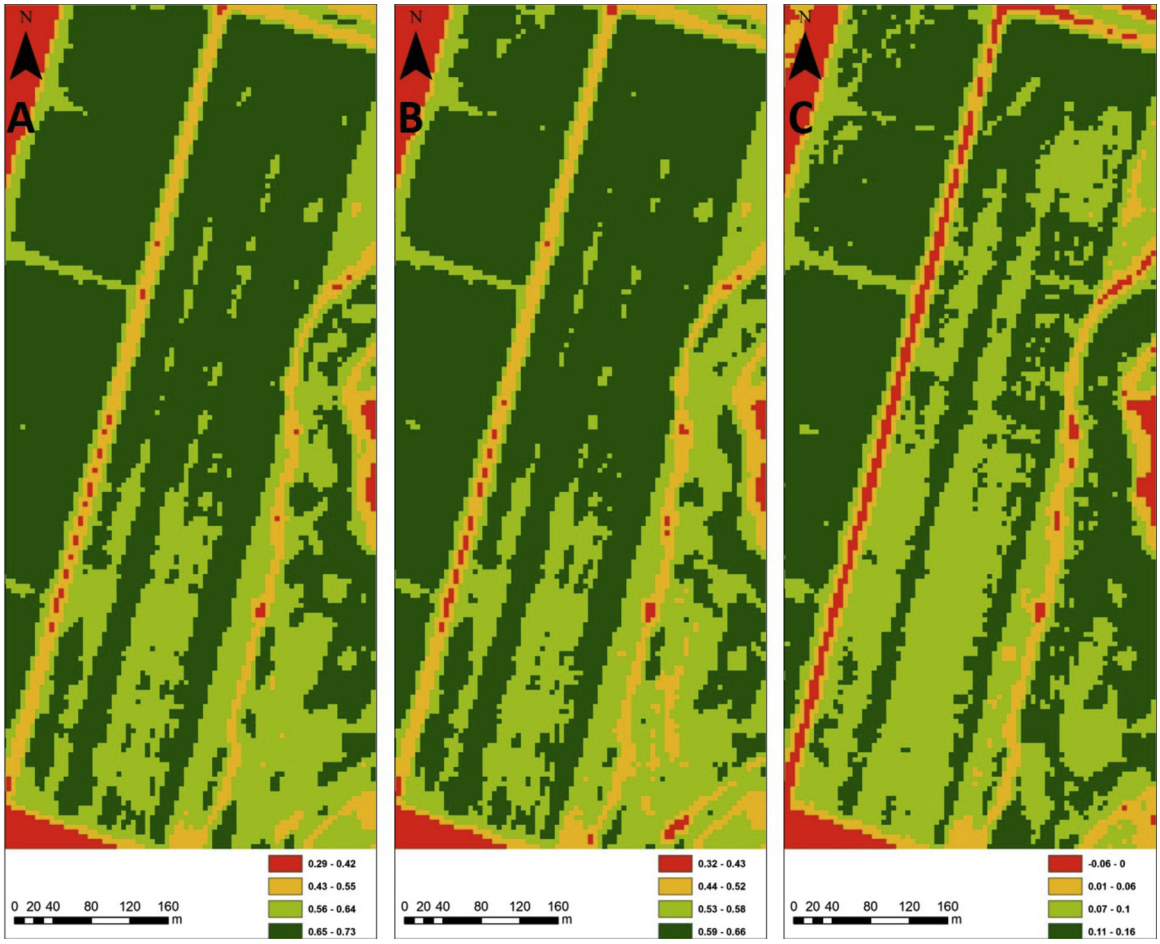

Fig. 8. NDVI (A); GNDVI (B); and GRVI (C) vegetation indexes based on a Venus imagery of the cotton field in Hagoshrim test site from 17/06/2018 (Comparable to Fig. 7A).

was also shown that the GRVI can be used to distinguish a plant's phenological stages. In fact, detecting early season and senescence is easy with GRVI: a GRVI lower than 0 indicates low plant's vigor, whereas a GRVI greater than zero, indicates strong plant vigor, corresponding to the mid-season plant phenological stage (Figs. 2–4). It was also concluded that the GRVI is better than the NDVI and GNDVI in detecting subtle disturbances in mid-season (Fig. 6). High-resolution RGB imaging can be utilized to monitor the uniformity of irrigation water application and to detect heterogeneity in field irrigation (Fig. 5). Since both the camera and the UAV used in this research are inexpensive and available and the current auto-pilot UAV guiding technologies ease the use of UAVs, the presented tools should be available for "on-the-spot" farming decision-making processes involving precision irrigation and irrigation management.

Author contributions

Conceptualization, Assaf Chen and Moshe Meron; Data curation, Valerie Orlov-Levin ; Formal analysis, Assaf Chen and Valerie Orlov-Levin ; Investigation, Valerie Orlov-Levin ; Methodology, Assaf Chen and Moshe Meron; Software, Assaf Chen and Valerie Orlov-Levin ; Writing – original draft, Assaf Chen; Writing – review & editing, Assaf Chen and Moshe Meron.

Funding

This study was supported by a Grant from the Upper Galilee Development Corporation.

Conflicts of interest

The authors declare no conflict of interest.

Acknowledgment

Special thanks to Dr. Onn Rabinovitz, Min. of Agriculture field crops advisor, for his valuable assistance.

References

Adamsen, F.J., Pinter, P.J., Barnes, E.M., LaMorte, R.L., Wall, G.W., Leavitt, S.W., Kimball, B.A., 1999. Measuring wheat senescence with a digital camera. Crop Sci. https://doi.org/10.2135/cropsci1999.0011183X003900030019x.

Campillo, C., Prieto, M.H., Daza, C., Moñino, M.J., García, M.I., 2008. Using digital images to characterize canopy coverage and light interception in a processing tomato crop. HortScience 43, 1780–1786.

Daughtry, C.S.T., Walthall, C.L., Kim, M.S., De Colstoun, E.B., McMurtrey Iii, J.E., 2000. Estimating corn leaf chlorophyll concentration from leaf and canopy reflectance. Remote Sens. Environ. 74, 229–239. https://doi.org/10.1016/S0034-4257(00)00113-9.

Eitel, J.U.H., Long, D.S., Gessler, P.E., Hunt, E.R., Brown, D.J., 2009. Sensitivity of ground-based remote sensing estimates of wheat chlorophyll content to variation in soil reflectance. Soil Sci. Soc. Am. J. 73, 1715. https://doi.org/10.2136/sssaj2008.0288.

Fortes, R., Millán, S., Prieto, M.H., Campillo, C., 2015. A methodology based on apparent electrical conductivity and guided soil samples to improve irrigation zoning. Precis. Agric. 16, 441–454. https://doi.org/10.1007/s11119-015-9388-7.

Gitelson, A., Kaufman, Y., Merzlyak, M., 1996. Use of a green channel in remote sensing of global vegetation from EOS-MODIS. Remote Sens. Environ. 58, 289–298. https://doi.org/10.1016/S0034-4257(96)00072-7.

Gitelson, A.A., Kaufman, Y.J., Stark, R., Rundquist, D., 2002. Novel algorithms for remote estimation of vegetation fraction. Remote Sens. Environ. 80, 76–87. https://doi.org/10.1016/S0034-4257(01)00289-9.

Gitelson, A.A., Viña, A., Ciganda, V., Rundquist, D.C., Arkebauer, T.J., 2005. Remote estimation of canopy chlorophyll content in crops. Geophys. Res. Lett. 32, 1–4. https://doi.org/10.1029/2005GL022688.

Green, S., McNaughton, K., Wünsche, J.N., Clothier, B., 2003. Modeling light interception and transpiration of apple tree canopies. Agron. J. 95, 1380. https://doi.org/10.2134/agronj2003.1380.

Haboudane, D., Miller, J.R., Pattey, E., Zarco-Tejada, P.J., Strachan, I.B., 2004. Hyperspectral vegetation indices and novel algorithms for predicting green LAI of crop canopies: modeling and validation in the context of precision agriculture. Remote Sens. Environ. 90, 337–352. https://doi.org/10.1016/j.rse.2003.12.013.

Haghverdi, A., Leib, B.G., Washington-Allen, R.A., Ayers, P.D., Buschermohle, M.J., 2015. Perspectives on delineating management zones for variable rate irrigation. Comput. Electron. Agric. 117, 154–167. https://doi.org/10.1016/j.compag.2015.06.019.

Hatfield, J.L., Gitelson, A.A., Schepers, J.S., Walthall, C.L., 2008. Application of spectral remote sensing for agronomic decisions. Agron. J. 100. https://doi.org/10.2134/agronj2006.0370c.

Huete, A.R., 1988. A soil-adjusted vegetation index (SAVI). Remote Sens. Environ. 25, 295–309. https://doi.org/10.1016/0034-4257(88)90106-X.

Hunt, E.R., Daughtry, C.S.T., Eitel, J.U.H., Long, D.S., 2011. Remote sensing leaf chlorophyll content using a visible band index. Agron. J. 103, 1090–1099. https://doi.org/10.2134/agronj2010.0395.

Hunt, E.R., Doraiswamy, P.C., McMurtrey, J.E., Daughtry, C.S.T., Perry, E.M., Akhmedov, B., 2012. A visible band index for remote sensing leaf chlorophyll content at the Canopy scale. Int. J. Appl. Earth Obs. Geoinf. 21, 103–112. https://doi.org/10.1016/j.jag.2012.07.020.

Johnson, R.S., Ayars, J., Trout, T., Mead, R., Phene, C., 2000. Crop coefficients for mature peach trees are well correlated with midday canopy light interception. Acta Hortic.

Jordan, C.F., 1969. Derivation of leaf-area index from quality of light on the forest floor. Ecology 50, 663–666. https://doi.org/10.2307/1936256.

Kanemasu, E.T., 1974. Seasonal canopy reflectance patterns of wheat, sorghum, and soybean. Remote Sens. Environ. 3, 43–47. https://doi.org/10.1016/0034-4257(74)90037-6.

Meron, M., Fuchs, M., Levin, I., Halel, R., Feuer, R., 1989. Evaluation of evapotranspiration by combining plant characteristics and meteorological information. Actahort. Org 278, 501–507.

Meron, M., Tsipris, J., Hetsroni, A., Cohen, S., 2006. Aerial photography and ground based equipment to evaluate crop cover for tree specific irrigation scheduling. In: Mulla, D. (Ed.), 8th International Conference on Precision Agriculture Minneapolis MN USA. pp. CD.

Motohka, T., Nasahara, K.N., Oguma, H., Tsuchida, S., 2010. Applicability of Green-Red Vegetation Index for remote sensing of vegetation phenology. Remote Sens. 2, 2369–2387. https://doi.org/10.3390/rs2102369.

Nahry, A.H.E., Ali, R.R., Baroudy, A.A.E., 2011. An approach for precision farming under pivot irrigation system using remote sensing and GIS techniques. Agric. Water Manag. 98, 517–531. https://doi.org/10.1016/j.agwat.2010.09.012.

Rouse, J.W., Hass, R.H., Schell, J.A., Deering, D.W., 1973. Monitoring vegetation systems in the Great Plains with ERTS. Third Earth Resources Technology Satellite (ERTS) Symposium 1. pp. 309–317. https://doi.org/citeulike-article-id:12009708.

Testa, G., Gresta, F., Cosentino, S.L., 2011. Dry matter and qualitative characteristics of alfalfa as affected by harvest times and soil water content. Eur. J. Agron. 34, 144–152. https://doi.org/10.1016/j.eja.2010.12.001.

Tucker, C.J., 1979. Red and photographic infrared linear combinations for monitoring vegetation. Remote Sens. Environ. 8, 127–150. https://doi.org/10.1016/0034-4257(79)90013-0.

Yoder, B.J., Waring, R.H., 1994. The normalized difference vegetation index of small Douglas-fir canopies with varying chlorophyll concentrations. Remote Sens. Environ. 49, 81–91. https://doi.org/10.1016/0034-4257(94)90061-2.

Zhang, L., Clarke, M.L., Steven, M.D., Jaggard, K.W., 2011. Spatial patterns of wilting in sugar beet as an indicator for precision irrigation. Precis. Agric. 12, 296–316. https://doi.org/10.1007/s11119-010-9177-2.